International Journal of Electrical and Power Engineering 5 (1): 54-61, 2011
ISSN: 1990-7958

Digital Current Control of Switched Reluctance Motor

[1]Zeki Omac, [2]Hasan Kurum and [3]Ahmet Hakan Selcuk
[1]Department of Electrics, Voccational High School, Bingol University, 12000 Bingol, Turkey
[2]Department of Electrical and Electronics Engineering, Faculty of Engineering,
Firat University, 23119 Elazig, Turkey
[3]Department of Medical Electronics, Vocataional And Technical High School,
Firat University, 23119 Elazig, Turkey

Abstract: In this study, the torque produced by a switched reluctance motor having 18 poles in stator and 12 poles in rotor is calculated by using Finite element method. 18/12 SRM is compared with 12/8 and 6/4 poles SRMs according to their radial forces acting on rotor poles. Closed loop current model of the SRM under interest is also built and simulation results are obtained by computer. Closed loop current control application of SRM is performed by using a TMS320LF2407A Digital Signal Processor (DSP). Simulation results of closed loop current control of the SRM are compared with experimental results.

Key words: Switched reluctance motor, finite element method, current control, closed loop, DSP, Turkey

INTRODUCTION

Switched Reluctance Motor (SRM) is a low cost motor since, it has no windings or magnets on its rotor. It has only simple windings on its stator. Having the capability of producing high torque and rotating at high speeds and high efficiency makes switched reluctance motors more preferable in industry (Lawrenson *et al*., 1980).

However, switched reluctance motor has disadvantages of acoustic noise and torque ripple. Actually all electrical machines make noise but noise produced by SRM is higher than other electric motor types (Wallace *et al*., 1990). Noise from electric machines has been investigated in detail and several noise sources have been determined (Cameron *et al*., 1992; Wu and Pollock, 1995; Pillay *et al*., 1995; Hayaashi and Miller, 1995; Colby *et al*., 1996; Pollock and Wu, 1997; Vijayraghavan and Krishnan, 1999; Sanada *et al*., 2000; Miller, 2002). Solutions have been suggested to reduce the noise according to its type (Sanada *et al*., 2000; Miller, 2002; Cai *et al*., 2003; Tang *et al*., 2003, 2005; Rasmussen *et al*., 2004; Srinivas and Arumugam, 2005). It has been agreed that the main sources of the noise produced by an SRM are the radial forces. Therefore, some investigators have tried to reduce radial forces by changing the geometry of SRM while other controlling the phase voltage or phase current electronically (Wu and Pollock, 1995; Sanada *et al*., 2000; Miller, 2002; Cai *et al*., 2003). It is possible to separate the attraction force exerted on the rotor poles by the excited stator poles into two components as normal and tangential in an SRM. Tangential component of the force produces torque but normal component cause an attraction between stator and rotor poles and vibrations and acoustic noise occur in stator. Another name of normal force is radial force. It is very difficult to measure the radial force experimentally. Because of salient pole geometries of stator and rotor and high magnetic saturation, analytical modelling is not simple. That is why, Finite element method is used to calculate electromagnetic forces of SRM.

The torque ripple of SRM causes noise and variations in speed. This is an unwanted situation for servomotor applications. In the literature, methods to minimize torque ripple have been presented (Husain and Hossain, 2005; Husain, 2002; Russa *et al*., 1998; Islam *et al*., 2003). In SRM, electromagnetic torque varies with the magnitude of current. By controlling phase current, torque ripple is minimized.

In this study, an SRM with 18 poles in stator and 12 poles in rotor is used. The purpose is to reduce noise by decreasing radial force. A Proportional Integral (PI) current controller which controls phase currents is also digitally designed to reduce torque ripple.

CALCULATION OF TORQUE AND RADIAL FORCE BY FINITE ELEMENT METHOD

The fundamental variable calculated by finite element method is magnetic vector potential. The relation between

Corresponding Author: Zeki Omac, Vocational High School, Department of Electrics, Bingol University, 12000 Bingol, Turkey

magnetic vector potential and current density in 2 dimensions can be expressed analytically as:

$$\frac{\partial \mathbf{A}}{\partial x}\left(\frac{1}{\mu}\frac{\partial \mathbf{A}}{\partial x}\right)+\frac{\partial \mathbf{A}}{\partial y}\left(\frac{1}{\mu}\frac{\partial \mathbf{A}}{\partial y}\right)=-\mathbf{J} \quad (1)$$

Where:
A = Magnetic vector potential
J = Current density
μ = Magnetic permeability

The shape and dimensions of SRM model under investigation is shown in Fig. 1. One phase of the motor is built by connecting the windings on opposite 6 poles of stator in series.

The purpose is to reduce cost by decreasing the number of semiconductor switches used to drive the motor by reducing the total number of phases to 3 and the greater total produced torque is obtained. In order to increase the accuracy in calculations of magnetic quantities in air gap between stator and rotor, the air gap is divided into smaller elements. In Finite element method, analysis of the SRM, the program ANSYS has been used. The Meshed model of SRM is shown in Fig. 2. In this model, there are 16645 elements and 16648 nodes. Due to the Dirichlet boundary conditions, zero vector potentials are given to the nodes at enough far away from the motor. Current densities applied to the phase windings are calculated for each phase current value.

Magnetic vector potentials and field distributions of SRM for rotor positions of 0-8, 10, 12, 14, 15° and phase currents of 2-5 and 6.5 A are calculated. Isolated copper wire of 0.65 mm diameter has been used to build the phase windings of the motor.

In Finite element method calculations, the B-H curve shown in Fig. 3 which has been determined experimentally is used.

The field distribution for θ = 6° rotor position calculated by Finite element method is given in Fig. 4. The torque produced by one phase of N_s/N_r = 18/12 poles SRM under investigation with respect to rotor position for 2-5 and 6.5 A current values have been calculated separately by Finite element method. Torque graphs

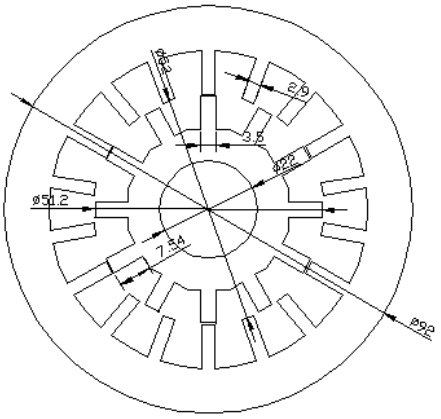

Fig. 1: Front view of the SRM under investigation

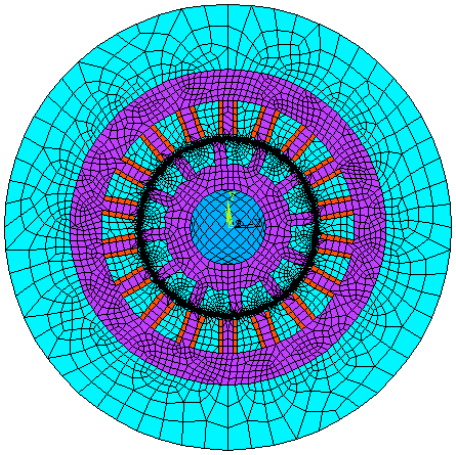

Fig. 2: The Meshed model of 18/12 poles SRM for θ = 6°

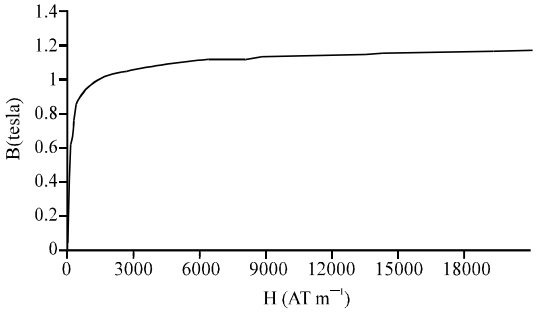

Fig. 3: Experimentally obtained B-H curve of plates used in the construction of stator and rotor of SRM

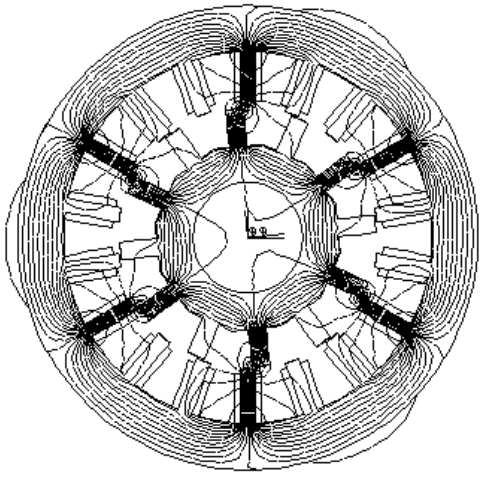

Fig. 4 The field distribution of 18/12 poles SRM for θ = 6°

obtained for different phase currents with respect to the rotor position are shown in Fig. 5 where, flux density is shown as vector in Fig. 6.

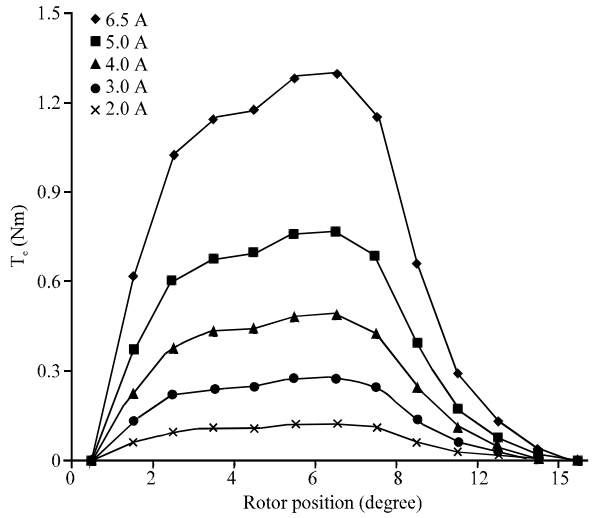

Fig. 5: The torque-position curve of 18/12 poles SRM calculated with FEM

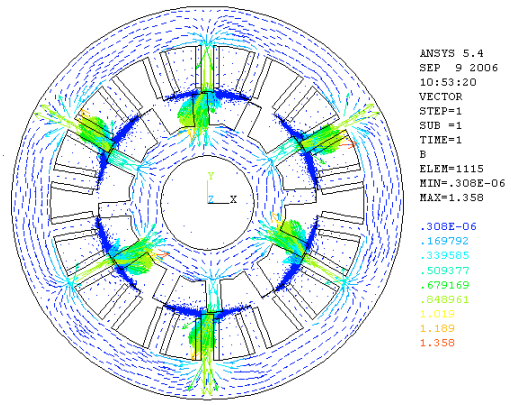

Fig. 6: The magnetic flux density distribution of 18/12 poles SRM under investigation for θ = 3° illustrated as vectors

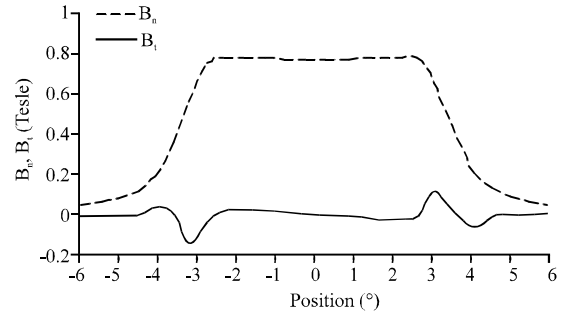

Fig. 7: Variations of the normal (B_n) and tangential (B_t) components of the air gap flux density

The variations of the components of the flux density with respect to rotor position for N_s/N_r = 18/12 poles SRM is shown in Fig. 7.

One of the fundamental problems with switched reluctance motor is noise caused by vibrations from radial forces. In this study, it is proved with three different SRM model that the radial force acting on a stator pole for the same peak value of torque is reduced when numbers of stator and rotor poles are increased. To be able to compare the results easily, motor structures that have the same number of phase, length, air gap width, inner and outer diameter of stator are chosen. Comparisons of radial forces acting on one rotor pole of three SRMs having different number of stator and rotor poles for the same peak value of torque are made as shown in Fig. 8.

Radial force acting on one rotor pole of SRMs having N_s/N_r = 6/4, 12/8 and 18/12 poles are calculated with the Finite element method (Omac, 2006). For all three types of motors, variations of radial forces with respect to rotor position are given in Fig. 9.

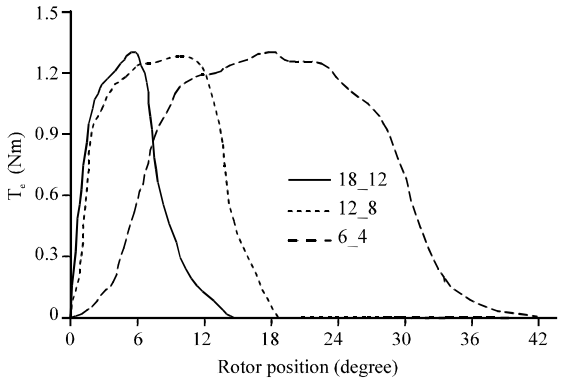

Fig. 8: Variations of torques with respect to the rotor positions for N_s/N_r = 18/12, 12/8 and 6/4 SRMs

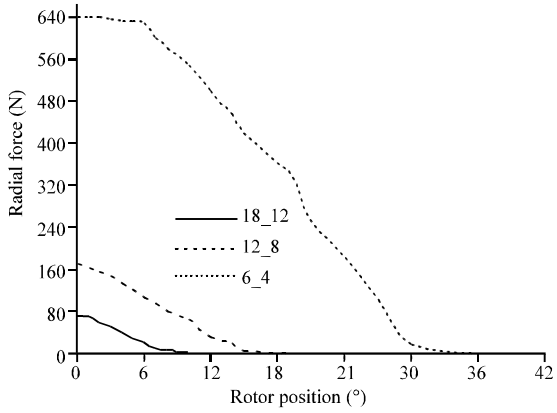

Fig. 9: The radial force variations with respect to the rotor position for N_s/N_r = 18/12, 12/8 and 6/4 SRMs

CURRENT CONTROL

Inductance is an important quantity in a SRM because the produced torque is dependent on the inductance. A positive torque is produced in the time period of increasing inductance where a negative torque occurs in the range of decreasing inductance. The variations of the phase inductances of the SRM under interest have been determined experimentally. Measured winding inductances of phases A-C are expressed mathematically as:

$$L_a = L_1 + L_2\cos(N_r\theta) \quad (2)$$

$$L_b = L_1 + L_2\cos(N_r\theta + \frac{2\pi}{3}) \quad (3)$$

$$L_c = L_1 + L_2\cos(N_r\theta - \frac{2\pi}{3}) \quad (4)$$

Where:

$$L_1 = \frac{1}{2}(L_{max} + L_{min}) \quad (5)$$

$$L_2 = \frac{1}{2}(L_{max} - L_{min}) \quad (6)$$

The voltage equation for one phase of SRM can be written as:

$$V = Ri + L\frac{di}{dt} + i\frac{dL}{d\theta}\omega \quad (7)$$

Where:

V = Line voltage
i = Phase current
R = Phase resistance
L = Phase inductance
θ = Angle
ω = Angular frequency

Here, there is a relation between angular position and angular velocity as:

$$\omega = \frac{d\theta}{dt} \quad (8)$$

Total torque produced by SRM is:

$$T_e = \sum_{j=1}^{m}\frac{1}{2}i_j^2\frac{dL_j(\theta, i)}{d\theta} \quad (9)$$

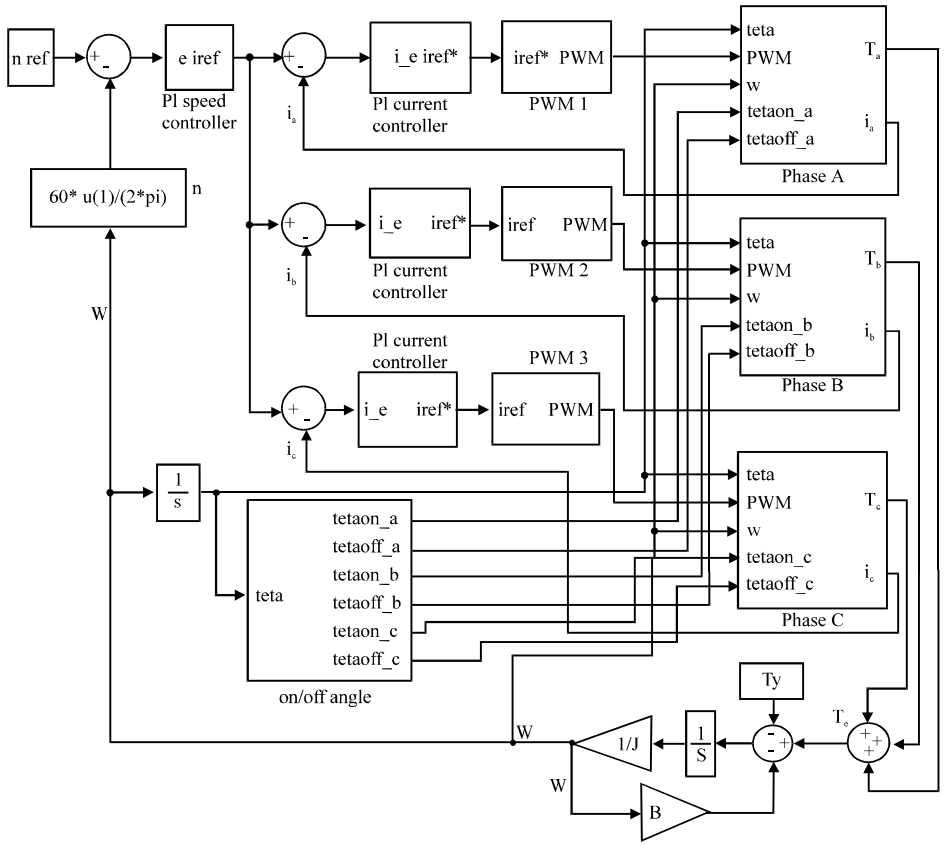

Fig. 10: The simulation diagram of closed loop current control of the SRM

Where:
T_e = Total torque
j = Phase index
m = No. of phases

The equation of movement can be written as:

$$T_e - T_l = J\frac{d\omega}{dt} + B\omega \quad (10)$$

Where:
T_l = Load torque
J = Inertia
B = Friction coefficient

To perform the closed loop current control of N_s/N_r = 18/12 poles SRM under investigation, the simulation diagram shown in Fig. 10 is built with Matlab/Simulink program. Other parameters used in simulation are as follows: phase resistance R = 2.6 Ω, inertia J = 0.000695 kg m^{-2}, friction coefficient B = 0.00018 Nm/rad/sec, peak value of the phase inductance L_{max} = 7.29 mH and the least value L_{min} = 2.36 mH.

Simulation and experimental results are obtained at 34 V line voltage and f = 15 kHz switching frequency. The proportional coefficient of PI is taken as K_p = 30 and integral coefficient K_i = 0.5 where initial value of integral K_c = 0 for current controller. IRG4BC30F IGBT transistors are used as switching elements in an asymmetric half bridge inverter having two switches per phase to drive the switched reluctance motor. To measure the phase currents, LTS 25-NP closed loop multi-level Hall sensor current detectors are used where IR110 integrated circuit is used to drive the IGBTs and a 360 pulses $cycle^{-1}$ shaft encoder is used to determine the rotor position. To control the SRM, TMS320LF2407A Digital Signal Processor (DSP) is chosen in this study. The operation frequency of TMS320LF2407A Digital Signal Processor (DSP) which is designed for motor control is 40 MHz and it is able to produce PWM signals at 20 kHz (Fig. 11). The DSP has 1610-bit A/D converters each having 375 ns cycle time. Current measurement information are given to DSP by using three inputs of A/D.

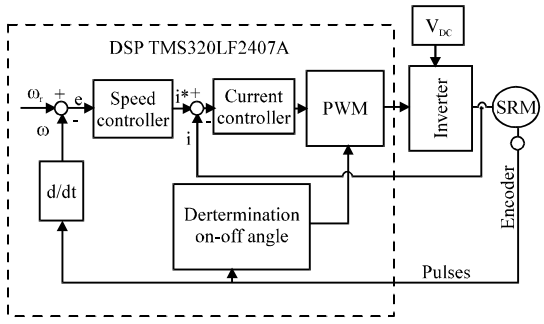

Fig. 11: The block diagram of closed loop current control application of switched reluctance motor with TMS320LF2407A Digital Signal Processor (DSP)

There are also four D/A placed on the EVM card. These outputs are used to see the phase currents on an oscilloscope screen. Also by using QEP circuit in DSP, the rotor speed and position is determined by means of the encoder pulses.

For closed loop control of speed and current of the motor, an assembly language program is developed by using the Code composer studio program developed by Texas instruments.

SIMULATION AND EXPERIMENTAL RESULTS

Speed graphics of simulation and experimental measurements of SRM driver under 0.46 Nm load and closed loop current control are shown in Fig. 12. The experiment set of the motor under investigation is shown in Fig. 13 where the photo of SRM driver circuit is shown in Fig. 14.

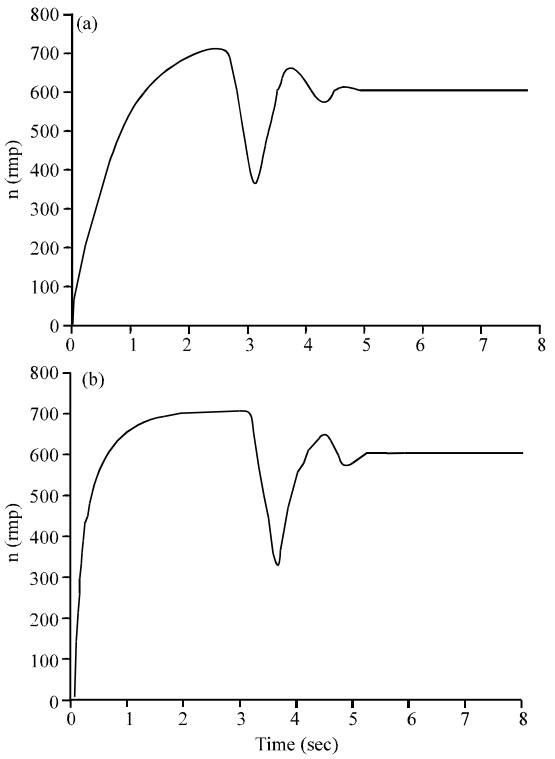

Fig. 12: a) Measured and b) Simulated graphic of i_a phase current variation of SRM driver under closed loop current control at n = 600 rpm rotor speed, V = 34 V driving voltage with T_l = 0.46 Nm load torque

Fig. 13: The photo illustrating switched reluctance motor, DC shunt generator and SR driver circuit set

Fig. 14: The photo of SRM driver circuit

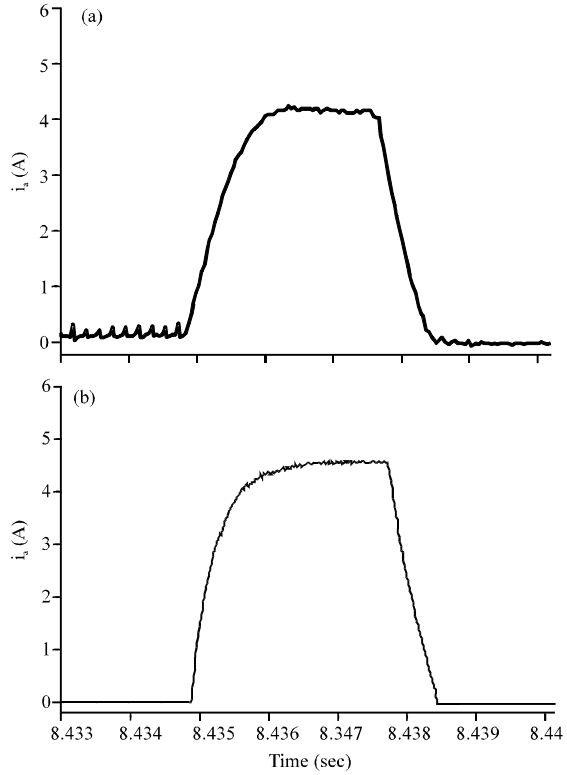

Fig. 15: a) Measured and b) Simulated graphic of i_a phase current variation of SRM driver under closed loop current control at n = 600 rpm rotor speed, V = 34 V driving voltage with T_l = 0.46 Nm load torque

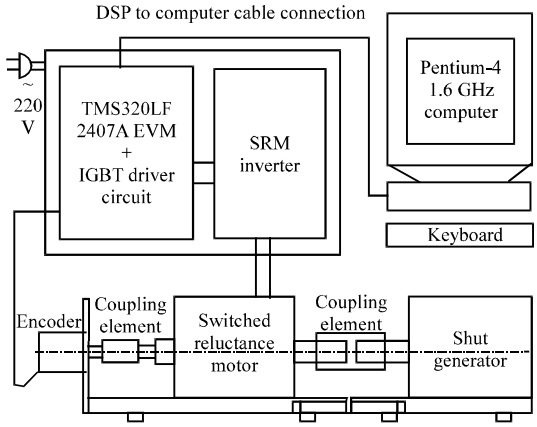

Fig. 16: Experimental connection diagram of SRM

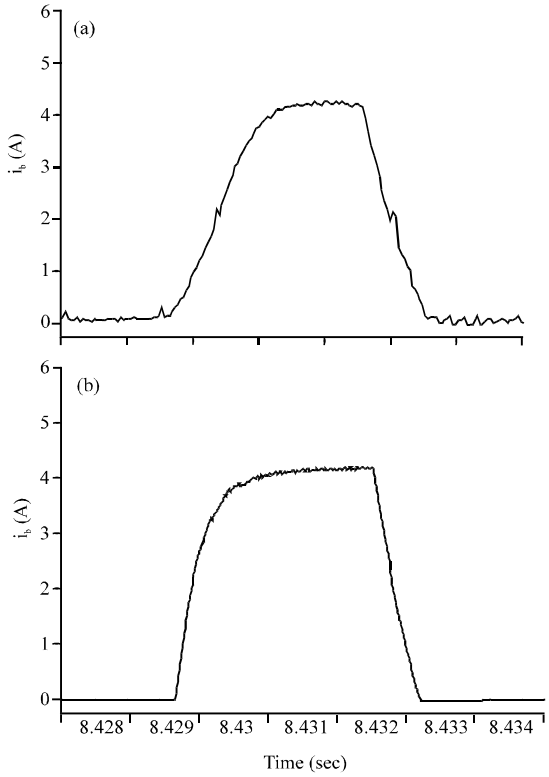

Fig. 17: a) Measured and b) Simulated graphic of i_b phase current variation of SRM driver under closed loop current control at n = 600 rpm rotor speed, V = 34 V driving voltage with T_l = 0.46 Nm load torque

Phase A current of SRM driver when the load torque T_y = 0.46 Nm with closed loop current control at n = 600 rpm reference speed measured in experiment and calculated by simulation is shown in Fig. 15, 16a and b while in Fig. 17a and b and in Fig. 18a and b.

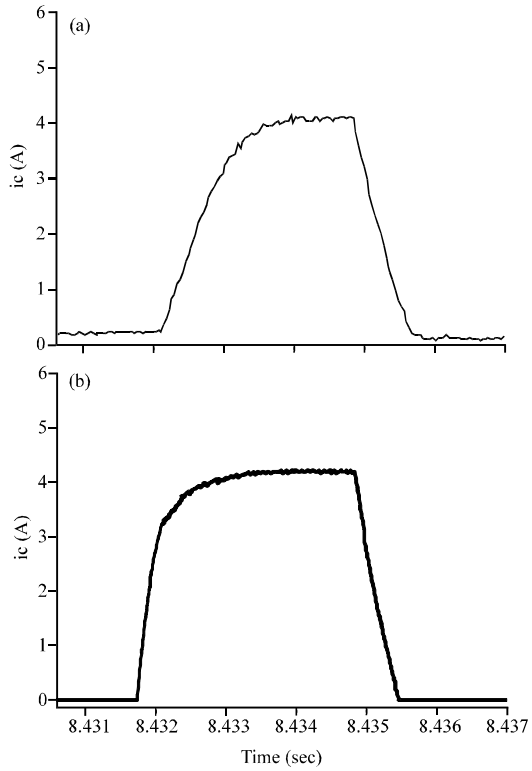

Fig. 18: a) Measured and b) Simulated graphic of i_c phase current variation of SRM driver under closed loop current control at n = 600 rpm rotor speed, V = 34 V driving voltage with T_l = 0.46 Nm load torque

CONCLUSION

N_s/N_r = 18/12 pole switched reluctance motor is investigated with finite element method. For the same peak value of torque as compared to 12/8 and 6/4 poles SRM model, it is determined from the calculation of radial force with finite element method that the least radial force acting on one rotor pole is produced in 18/12 poles SRM Also, the digital current control of 18/12 poles switched reluctance motor is performed. Simulation diagram of the SRM under investigation is built in computer and closed loop current control results are obtained under load. Closed loop current control of the SRM is performed by using TMS320LF2407A Digital Signal Processor (DSP) and experimental results are obtained. The accuracy of simulation results is satisfied with the experimental results.

NOMENCLATURE

L_{max} = Phase inductance at coinciding position
L_{min} = Phase inductance at non-coinciding position
N_r = Number of rotor poles
N_s = Number of stator poles
m = Number of phases
θ = Rotor position
R = Phase resistance
T_e = Total produced torque
V = Line voltage
J = Inertia
B = Friction coefficient
ω = Angular frequency
T_l = Load torque

REFERENCES

Cai, W., P. Pillay, Z. Tang and A.M. Omekanda, 2003. Low-vibration design of switched reluctance motors for automotive applications using modal analysis. IEEE Trans. Ind. Appl., 39: 971-977.

Cameron, D.E., J.H. Lang and S.D. Umans, 1992. The origin and reduction of acoustic noise in doubly salient variable-reluctance motors. IEEE Trans. Ind. Appl., 28: 1250-1255.

Colby, R.S., F.M. Mottier and T.J.E. Miller, 1996. Vibration modes and acoustic noise in a four-phase switched reluctance motor. IEEE Trans. Ind. Appl., 32: 1357-1364.

Hayaashi, Y. and T.J.E. Miller, 1995. A new approach to calculating core losses in the SRM. IEEE Trans. Ind. Appl., 31: 1039-1046.

Husain, I. and S.A. Hossain, 2005. Modeling, simulation and control of switched reluctance motor drives. IEEE Trans. Ind. Electron., 52: 1625-1634.

Husain, I., 2002. Minimization of torque ripple in SRM drives. IEEE Trans. Ind. Electron., 49: 28-39.

Islam, M.S., M.N. Anwar and I. Husain, 2003. Design and control of switched reluctance motors for wide-speed-range operation. IEEE Proc. Electr. Power Appl., 150: 425-430.

Lawrenson, P.J., J.M. Stephenson and P.T. Blenkinsop, 1980. Variable-speed switched reluctance motors. IEE Proc. B, Electr. Power Appl., 127: 253-265.

Miller, T.J.E., 2002. Optimal design of switched reluctance motors. IEEE Trans. Ind. Electron., 49: 15-27.

Omac, Z., 2006. Design of a new switched reluctance motor and its current control. Ph.D. Thesis, Firat University, Turkey.

Pillay, P., R.M. Samudio, M. Ahmed and R.T. Patel, 1995. A chopper-controlled SRM drive for reduced acoustic noise and improved ride-through capability using supercapacitors. IEEE Trans. Ind. Appl., 31: 1029-1038.

Pollock, C. and C.Y. Wu, 1997. Acoustic noise cancellation techniques for switched reluctance drivers. IEEE Trans. Ind. Appl., 33: 477-484.

Rasmussen, P.O., J.H. Andreasen and J.M. Pijanowski, 2004. Structural stator spacers-a solution for noise reduction of switched reluctance motors. IEEE Trans. Ind. Appl., 40: 574-581.

Russa, K., I. Husain and M.E. Elbuluk, 1998. Torque-ripple minimization in switched reluctance machines over a wide speed range. IEEE Trans. Ind. Appl., 34: 1105-1112.

Sanada, M., S. Morimoto, Y. Takeda and N. Matsui, 2000. Novel rotor pole design of switched reluctance motors to reduce the acoustic noise. Proceedings of the Industry Applications Conference, (IAC'00), Rome, pp: 107-113.

Srinivas, K.N. and R. Arumugam, 2005. Analysis and characterization of switched reluctance motors Part II flow thermal and vibration analyses. IEEE Trans. Magn., 41: 1321-1332.

Tang, Z., P. Pillay and A.M. Omekanda, 2003. Vibration prediction in switched reluctance motors with transfer function identification from shaker and force hammer tests. IEEE Trans. Ind. Appl., 39: 978-985.

Tang, Z., P. Pillay, Y. Chen and A.M. Omekanda, 2005. Prediction of electromagnetic forces and vibrations in SRMs operating at steady-state and transient speeds. IEEE Trans. Ind. Appl., 41: 927-934.

Vijayraghavan, P. and R. Krishnan, 1999. Noise in electric machines: A review. IEEE Trans. Ind. Appl., 35: 1007-1013.

Wallace, A.K., R. Sene and L.G. Martin, 1990. Current harmonics and acoustic noise in AC adjustable-speed drives. IEEE Trans. Ind. Appl., 26: 267-273.

Wu, C. and C. Pollock, 1995. Analysis and reduction of vibration and acoustic noise in the switched reluctance drive. IEEE Trans. Ind. Appl., 31: 91-98.